

AN INTERFACE CRACK IN PIEZOELECTRIC BIMATERIAL WITH ONE ELECTRICALLY CONDUCTIVE AND TWO ELECTRICALLY PERMEABLE ZONES AT ITS FACES

VOLODYMYR GOVORUKHA, MARC KAMLAH AND SHUO ZHAO

A mode III partially electroded interface crack between two different piezoelectric materials under the action of antiplane mechanical and in-plane electric loadings is analyzed. From the point of view of the boundary conditions on the crack faces, one zone of the crack faces in such crack can be considered as electrically conductive while the other parts are electrically permeable. Using special representations of field variables via sectionally analytic vector-functions, a homogeneous combined Dirichlet–Riemann boundary value problem is formulated. An exact analytical solution of this problem is obtained. Analytical expressions for the shear stress, electric field and also for the crack faces sliding displacement jump are derived. The intensity factors for stress and electric fields are determined as well. The dependencies of the mentioned values on the magnitude of the external electric loading and different ratios between the electrically conductive and electrically permeable crack face zone lengths are also demonstrated.

1. Introduction

It is well known that piezoelectric materials produce an electric field when deformed and undergo deformation when subjected to an electric field. Due to this intrinsic coupling effect, piezoelectric materials are widely used in design of various modern electromechanical devices, such as transducers, capacitors, sensors, and actuators. These smart devices often have a composite structure; therefore, because of the brittleness and the low strength of piezoelectric materials, interface delamination can appear during the manufacturing process or during service by impact electric and mechanical loadings. These delaminations can lead to interface cracks, which are the most dangerous kind of defects in such structures, and, therefore, it is a very important field of investigation.

In some cases, the stress-strain state occurring in the piezoelectric composites is related to antiplane deformation, which has stimulated an important theoretical effort for the investigation of piezoelectric composites operating in such conditions. In this light, a wealth of theoretical works has been devoted to the analysis of the interface antiplane shear cracks in piezoelectric materials. For example, antiplane problems for electrically permeable and impermeable cracks situated at the interface between piezoelectric layers or between a piezoelectric layer and an elastic layer were considered in [Narita and Shindo 1999; Soh et al. 2000; Kwon and Lee 2001; Li and Tang 2003a; 2003b; Wang and Sun 2004; Feng et al. 2011]. The papers [Chen et al. 1997; Fil'shtinskii and Fil'shtinskii 1997; Hou and Mei 1998; Gao and Wang 2001] are devoted to the consideration of the mode III interface crack problems for a piezoelectric compound subjected to piecewise uniform antiplane mechanical loading combined with in-plane electric loading at infinity. The antiplane problem of the collinear interface cracks between dissimilar piezoelectric

Keywords: antiplane problem, piezoelectric material, interface crack, field intensity factors.

materials subjected to electromechanical loading was studied in [Choi and Shin 2013; Choi and Chung 2013]. The problem of three-layer structure constructed of a piezoelectric and two elastic strips cracked at the interface was investigated in [Narita and Shindo 1998; Kwon and Lee 2000]. A moving antiplane crack between two dissimilar piezoelectric solids was analyzed in [Gao et al. 2001; Wang 2015; Nourazar and Ayatollahi 2016]. A more detailed review of antiplane crack problem investigation in piezoelectric composites was presented in the review paper [Govorukha et al. 2016].

Temporary actuators and other electronic devices are often constructed with use of the thin film electrodes embedded at a bimaterial interface. Such electrodes generally can be considered as metal films, which are more flexible than the surrounding piezoelectric materials. The delaminating of the mentioned electrodes or their debonding from the piezoelectric matrix is often observed. This leads to the appearance of the interface cracks with electroded faces. From the point of view of the boundary conditions on the crack faces, such cracks can be considered as electrically conductive cracks. For a plane case, a conductive interface crack in a piezoelectric bimaterial was considered in [Ru 2000; Beom and Atluri 2002; Häusler et al. 2004; Loboda et al. 2014]. Interfacial debonding and delamination between the embedded thin electrode and the piezoelectric matrix subjected to remote uniform antiplane shear stresses and in-plane electric fields was considered in [Govorukha et al. 2019]. It was assumed in this paper that all of the electrode region is electrically conducting and, additionally, that some part is delaminated. Wang and Zhong [2002], Wang et al. [2003], Lapusta et al. [2017], Onopriienko et al. [2019] studied an antiplane conductive crack at the interface between two dissimilar piezoelectric materials.

It should be mentioned that most results concerning the electrically conductive interface crack are related to the cases of one-type electric conditions on the crack faces. However, in many cases only some part of the crack faces can be conductive because of interface electrode delamination while on remaining part some other kind of electrical conditions can take place. This leads to a nontrivial mixed boundary value problem which becomes mathematically much more complicated than for uniform ones. In this paper, the analytical solution for a partially electroded interface crack under the action of antiplane mechanical and in-plane electric loadings is derived and some conclusions from the obtained solution are discussed.

2. Formulation of the problem and basic relations

Piezoelectric materials are approximately linear when an applied electric field or stress is small compared to the depolarization field. Thus, the stress σ_{ij} , strain γ_{ij} , electric displacement D_i , and electric field E_i obey the linear constitutive relations [Parton and Kudryavtsev 1988]

$$\sigma_{ij} = c_{ijkl}\gamma_{kl} - e_{kij}E_k, \quad D_i = e_{ikl}\gamma_{kl} + \varepsilon_{ik}E_k, \quad (1)$$

where c_{ijkl} , e_{ijk} and ε_{ij} are the elastic, piezoelectric and dielectric constants, respectively.

The governing field equations for a linear piezoelectric material in the absence of body forces and free electric charges are

$$\sigma_{ij,j} = 0, \quad D_{i,i} = 0, \quad (2)$$

where the subscript comma denotes partial derivative with respect to the Cartesian coordinates.

The expressions for the strain and electric fields have the form

$$\gamma_{ij} = \frac{1}{2}(u_{i,j} + u_{j,i}), \quad E_i = -\varphi_{,i}, \quad (3)$$

where u_i are the components of the elastic displacement vector and φ is the electric potential.

For the combined antiplane mechanical and in-plane electric loadings, assuming the material is transversely isotropic with a poling direction parallel to the x_3 -axis, one has

$$u_1 = u_2 = 0, \quad u_3 = u_3(x_1, x_2), \quad \varphi = \varphi(x_1, x_2).$$

Then the constitutive equations (1) can be further simplified and expressed as

$$\begin{Bmatrix} \sigma_{3j} \\ D_j \end{Bmatrix} = \begin{bmatrix} c_{44} & e_{15} \\ e_{15} & -\varepsilon_{11} \end{bmatrix} \begin{Bmatrix} \partial u_3 / \partial x_j \\ \partial \varphi / \partial x_j \end{Bmatrix}, \quad j = 1, 2, \quad (4)$$

and the governing field equations (2) become

$$\begin{aligned} c_{44} \nabla^2 u_3 + e_{15} \nabla^2 \varphi &= 0, \\ e_{15} \nabla^2 u_3 - \varepsilon_{11} \nabla^2 \varphi &= 0, \end{aligned} \quad (5)$$

where $\nabla^2 = \partial^2 / \partial x_1^2 + \partial^2 / \partial x_2^2$ is the two-dimensional Laplacian operator.

Assume further that the plane (x_1, x_2) consists of two piezoelectric half-planes $x_2 > 0$ and $x_2 < 0$ having different electromechanical properties. Then using equations (4) and (5) for each semi-infinite plane, and performing the analytic continuation procedure, similar to [Govorukha et al. 2019], one gets

$$\mathbf{v}^{(k)} = \mathbf{M}^{(k)} \mathbf{f}'^{(k)}(z) + \bar{\mathbf{M}}^{(k)} \bar{\mathbf{f}}'^{(k)}(\bar{z}), \quad (6)$$

$$\mathbf{p}^{(k)} = \mathbf{N}^{(k)} \mathbf{f}'^{(k)}(z) + \bar{\mathbf{N}}^{(k)} \bar{\mathbf{f}}'^{(k)}(\bar{z}), \quad (7)$$

where

$$\mathbf{v}^{(k)} = \left[\frac{\partial u_3^{(k)}}{\partial x_1}, D_2^{(k)} \right]^T, \quad \mathbf{p}^{(k)} = [\sigma_{23}^{(k)}, E_1^{(k)}]^T, \quad \mathbf{M}^{(k)} = \begin{bmatrix} 1 & 0 \\ i e_{15}^{(k)} & -i \varepsilon_{11}^{(k)} \end{bmatrix}, \quad \mathbf{N}^{(k)} = \begin{bmatrix} i c_{44}^{(k)} & i e_{15}^{(k)} \\ 0 & -1 \end{bmatrix},$$

and $k = 1$ stands for $x_2 > 0$ and $k = 2$ for $x_2 < 0$. The arbitrary vector-functions $\mathbf{f}^{(1)}(z)$ and $\mathbf{f}^{(2)}(z)$ of the complex variable $z = x_1 + i x_2$ are analytic in the upper and the lower half-planes, respectively.

Then, using the relations (6) and (7), the field variables at the bimaterial interface $x_2 = 0$, $|x_1| < \infty$ can be expressed via the limit values of the vector-function

$$\mathbf{w}(z) = \begin{cases} \mathbf{D} \mathbf{f}'^{(1)}(z) & \text{if } x_2 > 0, \\ -\bar{\mathbf{D}} \bar{\mathbf{f}}'^{(1)}(z) & \text{if } x_2 < 0, \end{cases}$$

in such a way that

$$\langle \mathbf{v}(x_1) \rangle = \mathbf{w}^+(x_1) - \mathbf{w}^-(x_1), \quad (8)$$

$$\mathbf{p}(x_1, 0) = \mathbf{G} \mathbf{w}^+(x_1) - \bar{\mathbf{G}} \mathbf{w}^-(x_1), \quad (9)$$

where $\mathbf{G} = \mathbf{N}^{(1)}(\mathbf{D})^{-1}$, $\mathbf{D} = \mathbf{M}^{(1)} - \bar{\mathbf{M}}^{(2)}(\bar{\mathbf{N}}^{(2)})^{-1} \mathbf{N}^{(1)}$ and the superscripts “+” and “-” indicate the limit values at the interface taken from the upper and the lower half-planes, respectively. Here and afterwards the brackets $\langle \dots \rangle$ denote the jump of the corresponding function over the bimaterial interface. Vector-function $\mathbf{w}(z) = [w_1(z), w_2(z)]^T$ is analytic in the whole complex plane, including the bonded parts of the bimaterial interface and tends to a constant as $|z| \rightarrow \infty$.

It is found out that for a bimaterial case and the considered transversely isotropic piezoelectric materials poled in the x_3 -direction, the matrix \mathbf{G} has the form

$$\mathbf{G} = \begin{bmatrix} ig_{11} & g_{12} \\ g_{21} & ig_{22} \end{bmatrix},$$

where all g_{kl} ($k, l = 1, 2$) are real.

The representations (8) and (9) can be used for solving antiplane problems for piezoelectric bimaterials with cracks at the interface. However, we transform these representations further to a form, which is more convenient for the solution of the mixed boundary value problem. Combining of the equations (8) and (9) leads to [Govorukha et al. 2019]

$$\sigma_{23}(x_1, 0) - im_1 E_1(x_1, 0) = t_1[F_1^+(x_1) + \gamma_1 F_1^-(x_1)], \quad (10)$$

$$\langle D_2(x_1) \rangle + is_1 \langle u_3'(x_1) \rangle = F_1^+(x_1) - F_1^-(x_1), \quad (11)$$

where

$$s_1 = \frac{g_{11} - m_1 g_{21}}{t_1}, \quad \gamma_1 = -\frac{g_{12} - m_1 g_{22}}{t_1}, \quad t_1 = g_{12} + m_1 g_{22},$$

$$m_1 = -\sqrt{-\frac{g_{11}g_{12}}{g_{21}g_{22}}}, \quad \frac{g_{11}g_{12}}{g_{21}g_{22}} < 0$$

and the function

$$F_1(z) = w_2(z) + is_1 w_1(z)$$

having the same properties as $\mathbf{w}(z)$.

Consider a crack $b_1 < x_1 < b_2$ located at the interface $x_2 = 0$ between two dissimilar piezoelectric half-planes $x_2 > 0$ and $x_2 < 0$, as shown in Figure 1. We suppose that outside the crack the half-planes are mechanically and electrically bonded along the interface and there are no traction and free charge on the crack surface. The upper and lower components of the bimaterial are piezoceramics with poling direction parallel to the x_3 -axis and material properties $c_{44}^{(k)}$, $e_{15}^{(k)}$, and $\varepsilon_{11}^{(k)}$, where the mentioned values are the stiffness, piezoelectric, and dielectric constants, respectively ($k = 1$ stands for the upper half-plane and $k = 2$ for the lower one). Assume that the part (a_1, a_2) of the interface crack faces is covered with electrodes. Since a thin film electrode is commonly much more flexible than the piezoelectric material, its mechanical properties are neglected. Thus, the electrodes are represented by their electrical properties, only. It means that the conditions on this section can be considered as electrically conductive. The remaining part of the crack is assumed to be free from electrodes. Therefore, because of the absence of the crack opening in x_2 direction this part of the crack faces should be considered as electrically permeable.

An antiplane mechanical loading σ_{23}^∞ and an in-plane electric loading E_1^∞ are applied at infinity. This loading results in an antiplane mechanical and in-plane electric state for which the relations (10) and (11) are valid. We will show in the following analysis that these relations are very convenient for the solution of interface crack problems with mixed boundary conditions at the crack faces.

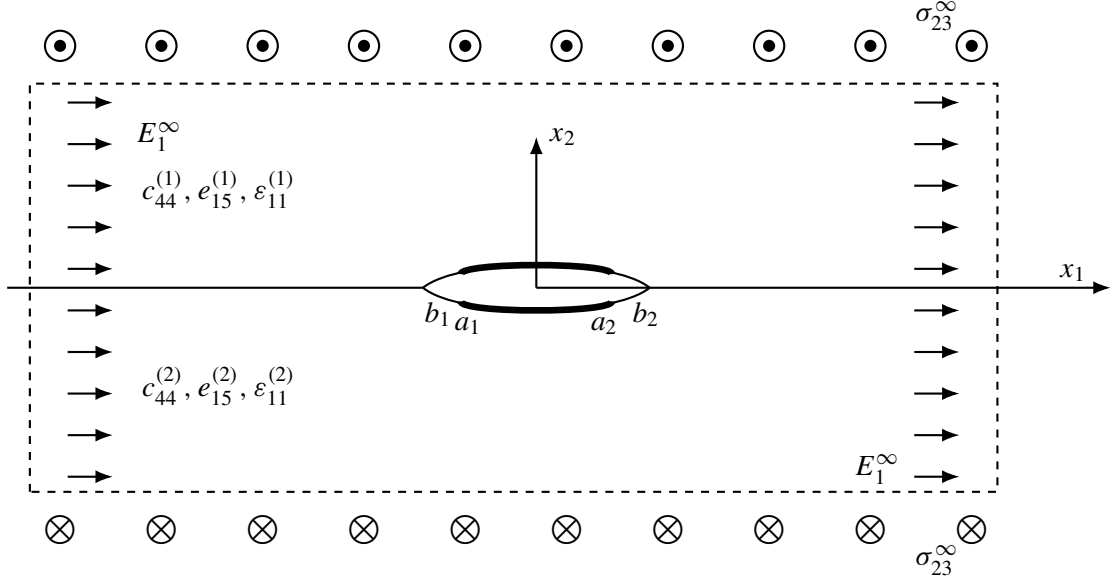


Figure 1. The partially electroded interface crack under the action of antiplane mechanical and in-plane electric loadings.

The electroded part of the crack is denoted by $L_a = (a_1, a_2)$, and the crack areas without electrode by $L_b = (b_1, a_1) \cup (a_2, b_2)$. Then the boundary conditions at the interface $x_2 = 0$ can be written as

$$\sigma_{23}^{(1)} = \sigma_{23}^{(2)} = 0, \quad E_1^{(1)} = E_1^{(2)} = 0, \quad x_1 \in L_a; \quad (12)$$

$$\sigma_{23}^{(1)} = \sigma_{23}^{(2)} = 0, \quad \langle D_2 \rangle = 0, \quad \langle E_1 \rangle = 0, \quad x_1 \in L_b; \quad (13)$$

$$\langle \sigma_{32} \rangle = 0, \quad \langle u_3 \rangle = 0, \quad \langle D_2 \rangle = 0, \quad \langle E_1 \rangle = 0, \quad x_1 \notin (b_1, b_2). \quad (14)$$

Using relations (10) and (11) and satisfying the boundary conditions (12)–(14), one gets

$$F_1^+(x_1) + \gamma_1 F_1^-(x_1) = 0, \quad x_1 \in L_a; \quad (15)$$

$$\operatorname{Re}[F_1^+(x_1) + \gamma_1 F_1^-(x_1)] = 0, \quad \operatorname{Re}[F_1^+(x_1) - F_1^-(x_1)] = 0, \quad x_1 \in L_b. \quad (16)$$

The simultaneous satisfaction of both equalities (16) leads to

$$\operatorname{Re} F_1^\pm(x_1) = 0, \quad x_1 \in L_b. \quad (17)$$

Introducing further the new function

$$\Phi_1(z) = -i F_1(z), \quad (18)$$

having the same properties as $F_1(z)$, the system (15), (17) can be written in the form

$$\Phi_1^+(x_1) + \gamma_1 \Phi_1^+(x_1) = 0, \quad x_1 \in L_a; \quad (19)$$

$$\operatorname{Im} \Phi_1^\pm(x_1) = 0, \quad x_1 \in L_b. \quad (20)$$

Taking into account that the function $\Phi_1(z)$ is analytic outside the crack, the conditions at infinity for the functions $\Phi_1(z)$ by using the prescribed remote electromechanical loads can be written as

$$\Phi_1(z)|_{z \rightarrow \infty} = \frac{\sigma_{23}^\infty - im_1 E_1^\infty}{it_1(1 + \gamma_1)}. \quad (21)$$

3. Solution of the problem

Equations (19) and (20) constitute a homogeneous combined Dirichlet–Riemann boundary value problem. The solution of such a problem concerning a rigid stamp was found in [Nakhmein and Nuller 1988] and, concerning an in-plane interface crack, it was developed in [Govorukha et al. 2017]. Using these results, the exact solution of the problem (19), (20) is presented in the Appendix.

Based on the obtained solution and the formulas (10), (11) and (18), one gets

$$\begin{aligned} \sigma_{23}(x_1, 0) &= -\frac{t_1(1 + \gamma_1)}{x_1 - d} \left[\frac{P(x_1) \sin \phi(x_1)}{\sqrt{(x_1 - a_1)(x_1 - a_2)}} + \frac{Q(x_1) \cos \phi(x_1)}{\sqrt{(x_1 - b_1)(x_1 - b_2)}} \right], \\ E_1(x_1, 0) &= -\frac{t_1(1 + \gamma_1)}{m_1(x_1 - d)} \left[\frac{P(x_1) \cos \phi(x_1)}{\sqrt{(x_1 - a_1)(x_1 - a_2)}} - \frac{Q(x_1) \sin \phi(x_1)}{\sqrt{(x_1 - b_1)(x_1 - b_2)}} \right] \end{aligned} \quad (22)$$

for $x_1 > b_2$,

$$\begin{aligned} \langle D_2(x_1) \rangle &= \frac{1 + \gamma_1}{\sqrt{\gamma_1}(x_1 - d)} \left[\frac{P(x_1) \cos \phi^*(x_1)}{\sqrt{(x_1 - a_1)(a_2 - x_1)}} - \frac{Q(x_1) \sin \phi^*(x_1)}{\sqrt{(x_1 - b_1)(b_2 - x_1)}} \right], \\ \langle u'_3(x_1) \rangle &= \frac{1 + \gamma_1}{s_1 \sqrt{\gamma_1}(x_1 - d)} \left[\frac{Q(x_1) \cos \phi^*(x_1)}{\sqrt{(x_1 - b_1)(b_2 - x_1)}} + \frac{P(x_1) \sin \phi^*(x_1)}{\sqrt{(x_1 - a_1)(a_2 - x_1)}} \right] \end{aligned} \quad (23)$$

for $x_1 \in (a_1, a_2)$, and

$$\begin{aligned} E_1(x_1, 0) &= -\frac{2t_1 \sqrt{\gamma_1} \cos[\pi h_2(x_1)]}{m_1(x_1 - d)} \left\{ \frac{P(x_1) \cosh[\tilde{\phi}(x_1) - \pi \varepsilon_1]}{\sqrt{(x_1 - a_1)(x_1 - a_2)}} + \frac{Q(x_1) \sinh[\tilde{\phi}(x_1) - \pi \varepsilon_1]}{\sqrt{(x_1 - b_1)(b_2 - x_1)}} \right\}, \\ \langle u'_3(x_1) \rangle &= \frac{2 \cos[\pi h_2(x_1)]}{s_1(x_1 - d)} \left[\frac{P(x_1) \sinh[\tilde{\phi}(x_1)]}{\sqrt{(x_1 - a_1)(x_1 - a_2)}} + \frac{Q(x_1) \cosh[\tilde{\phi}(x_1)]}{\sqrt{(x_1 - b_1)(b_2 - x_1)}} \right] \end{aligned} \quad (24)$$

for $x_1 \in (a_2, b_2)$, where

$$\begin{aligned} \phi^*(x_1) &= -Z(x_1) \left[\varepsilon_1 \int_{a_1}^{a_2} \frac{dt}{Z(t)(t - x_1)} + i \int_{b_1}^{a_1} \frac{h_1(t) dt}{Z^+(t)(t - x_1)} + i \int_{a_2}^{b_2} \frac{h_2(t) dt}{Z^+(t)(t - x_1)} \right], \\ \tilde{\phi}(x_1) &= -iZ^+(x_1) \left[\varepsilon_1 \int_{a_1}^{a_2} \frac{dt}{Z(t)(t - x_1)} + i \int_{b_1}^{a_1} \frac{h_1(t) dt}{Z^+(t)(t - x_1)} + i \int_{a_2}^{b_2} \frac{h_2(t) dt}{Z^+(t)(t - x_1)} \right]. \end{aligned}$$

Analysis of the formulas (22)–(24) shows that the stress $\sigma_{23}(x_1, 0)$ is singular for $x_1 \rightarrow b_2 + 0$, $E_1(x_1, 0)$ is singular for $x_1 \rightarrow a_2 + 0$ and $x_1 \rightarrow b_2 - 0$, and also $\langle D_2(x_1) \rangle$ is singular for $x_1 \rightarrow a_2 - 0$. Here, $x_1 \rightarrow b_2 + 0$ and $x_1 \rightarrow b_2 - 0$ denote approximation in the right-sided and left-sided neighborhood of b_2 , respectively. In all mentioned cases, inverse square root singularities are found. Thus, the intensity factors can be defined as

$$\begin{aligned} K_\sigma^{b_2} &= \lim_{x_1 \rightarrow b_2 + 0} \sqrt{2\pi(x_1 - b_2)} \sigma_{32}(x_1, 0), & K_E^{a_2} &= \lim_{x_1 \rightarrow a_2 + 0} \sqrt{2\pi(x_1 - a_2)} E_1(x_1, 0), \\ K_E^{b_2} &= \lim_{x_1 \rightarrow b_2 - 0} \sqrt{2\pi(b_2 - x_1)} E_1(x_1, 0), & K_D^{a_2} &= \lim_{x_1 \rightarrow a_2 - 0} \sqrt{2\pi(a_2 - x_1)} \langle D_2(x_1) \rangle. \end{aligned}$$

Applying the formulas of [Muskhelishvili 1953] to Cauchy type integrals, which are expressed via the functions $\tilde{\phi}(x_1)$, $\phi^*(x_1)$ and $\phi(x_1)$ in the vicinity of singular points, one arrives at

$$\phi(b_2) = 0, \quad \phi^*(a_2) = \pi, \quad \tilde{\phi}(a_2) = \pi \varepsilon_1.$$

Substituting these formulas into (22) and (24) and considering the obtained expressions in the vicinity of the points a_2 and b_2 , we get

$$K_\sigma^{b_2} = -\frac{t_1(1+\gamma_1)\sqrt{2\pi}}{b_2-d} \frac{Q(b_2)}{\sqrt{b_2-b_1}}, \quad K_E^{a_2} = \frac{2t_1\sqrt{2\pi}\gamma_1}{m_1(a_2-d)} \frac{P(a_2)}{\sqrt{a_2-a_1}}. \quad (25)$$

The intensity factors $K_E^{b_2}$ and $K_D^{a_2}$ can be found via the relations (25) in the form

$$K_E^{b_2} = \frac{1-\gamma_1}{m_1(1+\gamma_1)} K_\sigma^{b_2}, \quad K_D^{a_2} = -\frac{m_1(1+\gamma_1)}{2t_1\gamma_1} K_E^{a_2}. \quad (26)$$

4. Numerical results and discussion

Numerical analysis has been performed for a bimaterial composed of commercially available piezoelectric ceramics PZT-4 (the upper material) and PZT-5H (the lower one). The material properties of these materials are taken from [Park and Sun 1995] and [Pak 1992], respectively, and $\sigma_{23}^\infty = 1$ MPa, $b_2 - b_1 = 20$ mm are chosen for all calculations presented here. The analytical solution is obtained for any positions of the points a_1 and a_2 . However, for the sake of clarity of the numerical illustrations it is assumed in this section that the centers of the intervals (b_1, b_2) and (a_1, a_2) coincide with each other. Numerical results are presented for different ratios $\omega = (a_2 - a_1)/(b_2 - b_1)$. The main attention of the following numerical analysis will be devoted to the influence of the external electrical loading on the stress and electric field intensity factors, the crack faces sliding displacement jump along the crack region and the spatial variations of the field variables at the bimaterial interface.

At the beginning, the variations of the crack faces sliding displacement jump, i.e., the jump $\langle u_3(x_1) \rangle$ along the crack region (b_1, b_2) , are calculated and presented in Figure 2 for $\omega = 0.8$ and $\omega = 0.4$. It is clearly seen from these results that the crack faces sliding displacement jump is almost symmetrical for $E_1^\infty = 0$, but nonzero values of E_1^∞ leads to the distortion of the graphs and even to the change of the sign of $\langle u_3(x_1) \rangle$ at some part of the crack. However, the appearance of a negative sign of $\langle u_3(x_1) \rangle$ does not mean crack faces interpenetration like in the plane case because of the normal displacement and, instead, is well admissible from physical point of view for the present antiplane case. The obtained results demonstrate a strong influence of electrical loading upon the crack sliding at the points a_1 and a_2 , dividing the electrically conducting and electrically permeable crack face regions. The maximum of the crack faces sliding displacement jump increases as the electric field increases. It is also worth mentioning that the change of the sign of electric field E_1^∞ leads to mirror mapping of the obtained graphs with respect to the x_2 -axis.

The variation of the electric field $E_1(x_1, 0)$ along the electrically permeable crack region (a_2, b_2) is shown in Figure 3 for $\omega = 0.8$ and $\omega = 0.4$. It is seen from these figures that $E_1(x_1, 0)$ is almost equal to 0 for $E_1^\infty = 0$, but it becomes rather large for a nonzero external electric field. Besides, $E_1(x_1, 0)$ is singular at both ends of the segment (a_2, b_2) .

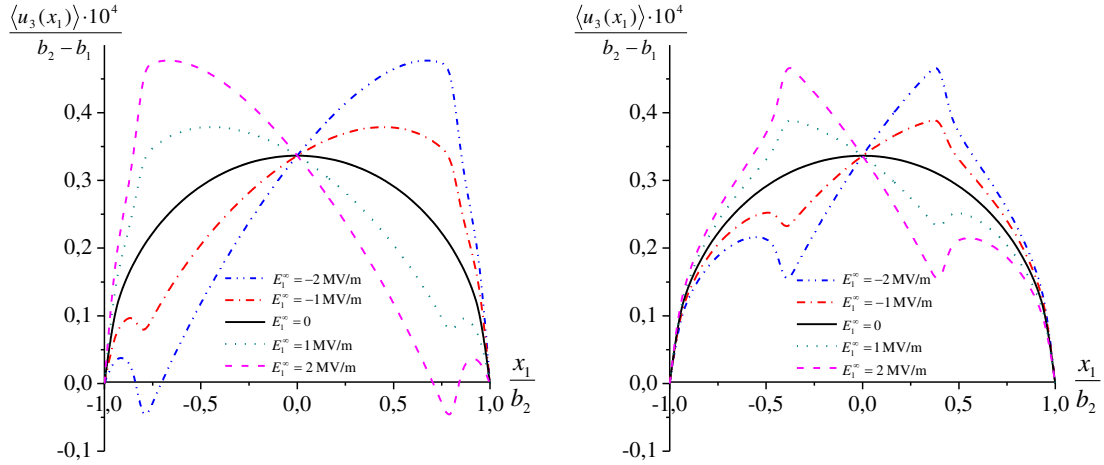


Figure 2. The variation of the normalized crack faces sliding displacement jump along the crack region for $\omega = 0.8$, left, and $\omega = 0.4$, right, and different values of E_1^∞ (the solid lines correspond to the absence of the external electric field).

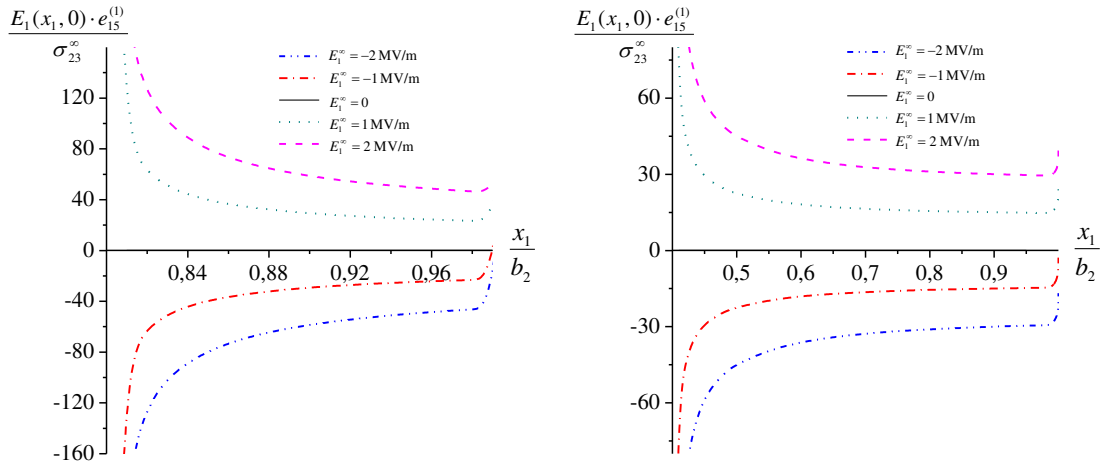


Figure 3. Variation of the electric field $E_1(x_1, 0)$ along the electrically permeable crack region (a_2, b_2) for the same values of ω and E_1^∞ as in Figure 2.

Figure 4 shows the variations of the shear stress $\sigma_{23}(x_1, 0)$ at the crack continuation $x_1 > b_2$ for $\omega = 0.8$ and $\omega = 0.4$. These figures confirm the analytical conclusion that the shear stress $\sigma_{23}(x_1, 0)$ grows to infinity for $x_1 \rightarrow b_2 + 0$ and tends to its nominal value for all x_1 much larger than the crack length. Thus, it is observed from these figures that the value of $\sigma_{23}(x_1, 0)$ decreases with the increase in magnitude of the applied electrical loading, however, this dependence is rather small.

Figure 5 displays the variation of the shear stress $\sigma_{23}(x_1, 0)$ and the electric field $E_1(x_1, 0)$ in the right neighboring area of the crack tip b_2 for different values of ω , where $E_1^\infty = -2 \text{ MV/m}$. It can be seen that the shear stress $\sigma_{23}(x_1, 0)$ and the electric field $E_1(x_1, 0)$ vary essentially with respect to the length of the electrically permeable zones. In addition, we verify some of the obtained results. Taking

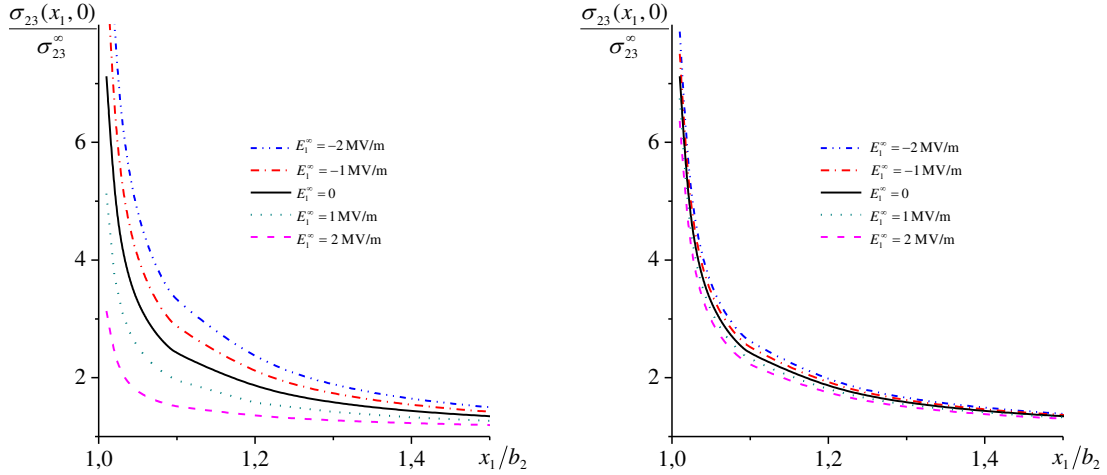


Figure 4. Variation of the stress $\sigma_{23}(x_1, 0)$ along the crack continuation $x_1 > b_2$ for $\omega = 0.8$, left, and $\omega = 0.4$, right, and different values of E_1^∞ .

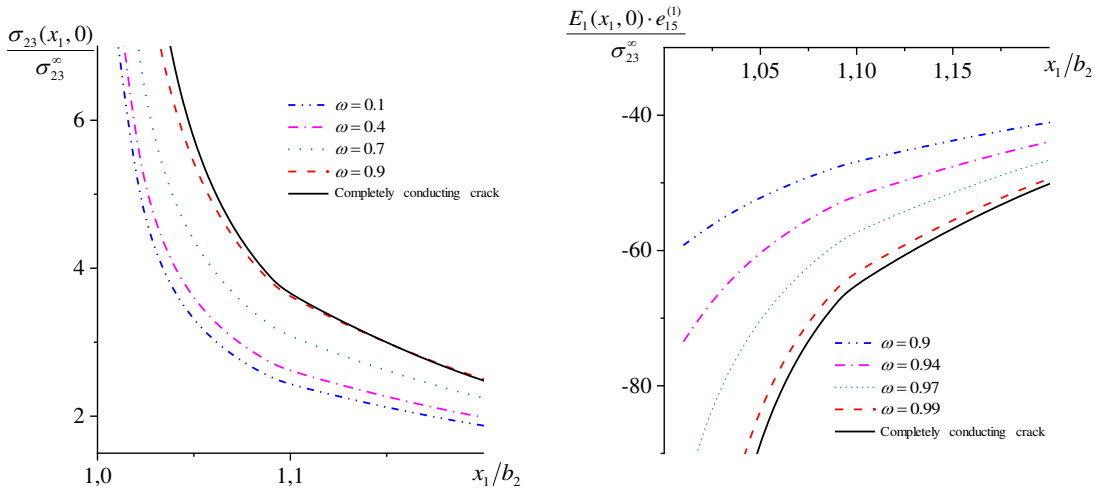


Figure 5. Variation of the shear stress $\sigma_{23}(x_1, 0)$, left, and the electric field $E_1(x_1, 0)$, right, in the right neighboring area of the crack tip b_2 for different values of ω .

into account that an available benchmark solution for a partially electroded interface crack could not be found in the literature, the comparison was performed with the values, obtained on the associated formulas of [Wang et al. 2003] for the extremely low speed regime ($V = 0$). It follows from the presented results that the curves for the case of mixed electrical conditions (dashed lines) tend to the curves of the completely electrically conducting interface crack (solid lines) while ω tends to 1. Moreover, with further approach of a_k to b_k ($k = 1, 2$) the corresponding curves completely coincide. This tendency and the validity of the results for a completely electrically conducting interface crack confirm the correctness of the derived solutions.

E_1^∞ [V/m]	$K_\sigma^{b_2}$ [Pa $\sqrt{\text{m}}$]		$K_E^{a_2}$ [V/ $\sqrt{\text{m}}$]	
	$\omega = 0.8$	$\omega = 0.4$	$\omega = 0.8$	$\omega = 0.4$
$-1 \cdot 10^8$	$5.4065 \cdot 10^6$	$1.1524 \cdot 10^6$	$-1.5850 \cdot 10^7$	$-1.1210 \cdot 10^7$
$-1 \cdot 10^6$	$2.2953 \cdot 10^5$	$1.8699 \cdot 10^5$	$-1.5839 \cdot 10^5$	$-1.1207 \cdot 10^5$
$-1 \cdot 10^4$	$1.7776 \cdot 10^5$	$1.7734 \cdot 10^5$	$-1.4767 \cdot 10^3$	$-1.0924 \cdot 10^3$
$-6.8357 \cdot 10^2$	$1.7727 \cdot 10^5$	$1.7725 \cdot 10^5$	≈ 0	-48.055
$-2.5488 \cdot 10^2$	$1.7725 \cdot 10^5$	$1.7724 \cdot 10^5$	67.947	≈ 0
$-1 \cdot 10^2$	$1.7724 \cdot 10^5$	$1.7724 \cdot 10^5$	92.495	17.361
0	$1.7724 \cdot 10^5$	$1.7724 \cdot 10^5$	$1.0835 \cdot 10^2$	28.571
$1 \cdot 10^2$	$1.7723 \cdot 10^5$	$1.7724 \cdot 10^5$	$1.2420 \cdot 10^2$	39.781
$1 \cdot 10^4$	$1.7671 \cdot 10^5$	$1.7715 \cdot 10^5$	$1.6933 \cdot 10^3$	$1.1495 \cdot 10^3$
$1 \cdot 10^6$	$1.2494 \cdot 10^5$	$1.6749 \cdot 10^5$	$1.5861 \cdot 10^5$	$1.1213 \cdot 10^5$
$3.3894 \cdot 10^6$	≈ 0	$1.4419 \cdot 10^5$	$5.3733 \cdot 10^5$	$3.7997 \cdot 10^5$
$1.8175 \cdot 10^7$	$-7.7317 \cdot 10^5$	≈ 0	$2.8808 \cdot 10^6$	$2.0374 \cdot 10^6$
$1 \cdot 10^8$	$-5.0520 \cdot 10^6$	$-7.9795 \cdot 10^5$	$1.5850 \cdot 10^7$	$1.1210 \cdot 10^7$

Table 1. The variations of stress and electric field intensity factors for different intensities of the external electric field

The variations of the stress intensity factor $K_\sigma^{b_2}$ and of the electric field intensity factor $K_E^{a_2}$ are shown in Table 1 for different values of ω and E_1^∞ . It can be seen that the dependence of both $K_\sigma^{b_2}$ and $K_E^{a_2}$ on the external electrical loading is rather significant. For each ω , the growing of electric field E_1^∞ leads to decreasing of the stress intensity factor $K_\sigma^{b_2}$ and, eventually, even reduces it to zero. It means that growing E_1^∞ decreases the danger of the crack development. On the other hand, the electric field intensity factor $K_E^{a_2}$ is approximately proportional to the external electric field for large values of this field.

5. Conclusion

A partially electroded interface crack between two semi-infinite piezoelectric planes under the action of antiplane mechanical and in-plane electric loadings has been analyzed. Such a crack can arise, e.g., in case of exfoliations of electrodes. Using representations (10), (11) of the field variables by means of piecewise analytic functions, the problem is reduced to a homogeneous combined Dirichlet–Riemann boundary value problem (19), (20) with the condition (21) at infinity, and its exact analytical solution is derived. The crack faces sliding displacement jumps, the electric field and the shear stress are calculated along the corresponding parts of the material interface for different values of the external electric loading and different ratios between the electrically conductive and electrically permeable crack face zone lengths. Furthermore, the stress and electric field intensity factors are found in closed form. It follows from the obtained results that the growth of the external electric field leads to a decrease in the stress intensity factor at the crack tips and to an increase in the electric field intensity factor at the points dividing the electrically conductive and electrically permeable zones of the crack.

Appendix

The solution of the homogeneous combined Dirichlet–Riemann boundary value problem (19), (20) satisfying the condition at infinity (21) as well as the condition of unique displacement and absence of an electric charge in the crack region [Govorukha et al. 2019] is given by

$$\Phi_1(z) = X(z)[P(z) + iY(z)Q(z)],$$

where

$$X(z) = \frac{e^{i\phi(z)}}{(z-d)\sqrt{(z-a_1)(z-a_2)}}, \quad Y(z) = \sqrt{\frac{(z-a_1)(z-a_2)}{(z-b_1)(z-b_2)}},$$

$$\phi(z) = -Z(z) \left(\varepsilon_1 \int_{a_1}^{a_2} \frac{dt}{Z^+(t)(t-z)} + i \int_{b_1}^{a_1} \frac{h_1(t) dt}{Z^+(t)(t-z)} + i \int_{a_2}^{b_2} \frac{h_2(t) dt}{Z^+(t)(t-z)} \right), \quad \varepsilon_1 = \frac{\ln \gamma_1}{2\pi},$$

$$Z(z) = \sqrt{(z-a_1)(z-a_2)(z-b_1)(z-b_2)}, \quad h_1(x_1) = n^*, \quad h_2(x_1) = \begin{cases} 1 & \text{if } x_1 \in (a_2, d), \\ 0 & \text{if } x_1 \in (d, b_2), \end{cases}$$

n^* is an integer number, and $d \in (a_2, b_2)$ is the pole of the function $X(z)$.

The integrals in the expression for the function $\phi(z)$ can be represented via elliptic integrals as

$$\phi(z) = \frac{-2}{\sqrt{(b_2-a_1)(a_2-b_1)}} \left\{ \varepsilon_1 \sqrt{\frac{(z-a_2)(z-b_2)}{(z-a_1)(z-b_1)}} \phi_1(z) + n^* \sqrt{\frac{(z-a_1)(z-a_2)}{(z-b_1)(z-b_2)}} \phi_2(z) - \sqrt{\frac{(z-b_1)(z-b_2)}{(z-a_1)(z-a_2)}} \phi_3(z) \right\},$$

where

$$\begin{aligned} \phi_1(z) &= (a_1 - b_1)\Pi(p_1, q) + (z - a_1)K(q), & p_1 &= p_1^* \frac{z-b_1}{z-a_1}, & p_1^* &= \frac{a_2-a_1}{a_2-b_1}, \\ \phi_2(z) &= (b_1 - b_2)\Pi(p_2, r) + (z - b_1)K(r), & p_2 &= p_2^* \frac{z-b_2}{z-b_1}, & p_2^* &= \frac{b_1-a_1}{b_2-a_1}, \\ \phi_3(z) &= (a_2 - a_1)\Pi(\mu, p_3, r) + (z - a_2)F(\mu, r), & p_3 &= p_3^* \frac{z-a_1}{z-a_2}, & p_3^* &= \frac{b_2-a_2}{b_2-a_1}, \\ q &= \sqrt{\frac{(a_2-a_1)(b_2-b_1)}{(b_2-a_1)(a_2-b_1)}}, & r &= \sqrt{\frac{(b_2-a_2)(a_1-b_1)}{(b_2-a_1)(a_2-b_1)}}, & \mu &= \arcsin \sqrt{\frac{(b_2-a_1)(d-a_2)}{(b_2-a_2)(d-a_1)}}. \end{aligned}$$

Here, $F(\mu, r)$ and $\Pi(\mu, p, r)$ are incomplete elliptic integrals of the first and third kind, while $K(r)$ and $\Pi(p, r)$ are complete elliptic integrals of the first and third kind.

The expansion of function $\phi(z)$ at infinity has the form

$$\phi(z)|_{z \rightarrow \infty} = A_1 z + (A_2 + \xi_1 A_1) + (A_3 + \xi_1 A_2 + \xi_2 A_1) z^{-1} + O(z^{-2}),$$

where

$$A_j = \varepsilon_1 \int_{a_1}^{a_2} \frac{t^{j-1} dt}{Z(t)} + i \int_{b_1}^{a_1} \frac{t^{j-1} h_1(t) dt}{Z^+(t)} + i \int_{a_2}^{b_2} \frac{t^{j-1} h_2(t) dt}{Z^+(t)}, \quad j = 1, 2, 3.$$

The integer n^* and the pole d can be found from the condition of finite values at infinity of the function $\phi(z)$ as

$$-\varepsilon_1 \frac{K(q)}{K(r)} < n^* < 1 - \varepsilon_1 \frac{K(q)}{K(r)}, \quad d = \frac{a_1(b_2 - a_2)sn^2(\omega, r) - a_2(b_2 - a_1)}{(b_2 - a_2)sn^2(\omega, r) - (b_2 - a_1)},$$

where $sn(\omega, r)$ is the Jacobi elliptic function and $\omega = \varepsilon_1 K(q) + n^* K(r)$.

The functions $P(z)$ and $Q(z)$, appearing in the solution, have the form

$$P(z) = C_0 + C_1 z + C_2 z^2, \quad Q(z) = D_0 + D_1 z + D_2 z^2,$$

where

$$C_0 = -C_1 \left(d - \frac{\chi}{\chi^*} \right) - d C_2 \left(d - \frac{2\chi}{\chi^*} \right) - \frac{\chi^2}{\chi^*} (D_1 + 2d D_2),$$

$$D_0 = \frac{1}{\chi^*} (C_1 + 2d C_2) - D_1 \left(d + \frac{\chi}{\chi^*} \right) - d D_2 \left(d + \frac{2\chi}{\chi^*} \right),$$

$$C_1 = \alpha_1 D_2 - \nu_1 C_2, \quad D_1 = -(\nu_1 + \eta_1) D_2 - \alpha_1 C_2,$$

$$C_2 = -\frac{m_1 E_1^\infty}{t_1(1 + \gamma_1)} \cos \alpha_0 - \frac{\sigma_{32}^\infty}{t_1(1 + \gamma_1)} \sin \alpha_0, \quad D_2 = \frac{m_1 E_1^\infty}{t_1(1 + \gamma_1)} \sin \alpha_0 - \frac{\sigma_{32}^\infty}{t_1(1 + \gamma_1)} \cos \alpha_0,$$

$$\chi = \sqrt{\frac{(d - a_1)(d - a_2)}{(d - b_1)(b_2 - d)}},$$

$$\chi^* = \frac{1}{2\chi} \left[\frac{(2d - a_1 - a_2)(d - b_1)(b_2 - d) + (2d - b_1 - b_2)(d - a_1)(d - a_2)}{(d - b_1)^2(b_2 - d)^2} \right],$$

$$\eta_1 = -\frac{1}{2}(a_1 + a_2 - b_1 - b_2), \quad \nu_1 = \frac{a_1 + a_2}{2} + d, \quad \alpha_0 = A_2, \quad \alpha_1 = A_3 + \xi_1 A_2.$$

Acknowledgments

This work was supported by the 2021 ‘‘Belt and Road’’ innovative talent exchange foreign expert project No. DL2021003002.

References

- [Beom and Atluri 2002] H. G. Beom and S. N. Atluri, ‘‘Conducting cracks in dissimilar piezoelectric media’’, *Int. J. Fract.* **118** (2002), 285–301.
- [Chen et al. 1997] Z.-T. Chen, S. W. Yu, and B. L. Karihalo, ‘‘Anti-plane shear problem for a crack between two dissimilar piezoelectric materials’’, *Int. J. Fract.* **86** (1997), L9–L14.
- [Choi and Chung 2013] S. R. Choi and I. Chung, ‘‘Analysis of three collinear antiplane interfacial cracks in dissimilar piezoelectric materials under non-self equilibrated electromechanical loadings on a center crack’’, *J. Mech. Sci. Technol.* **27** (2013), 3097–3101.
- [Choi and Shin 2013] S. R. Choi and J. K. Shin, ‘‘Three collinear antiplane interfacial cracks in dissimilar piezoelectric materials’’, *Int. J. Fract.* **179** (2013), 237–244.

- [Feng et al. 2011] F.-X. Feng, K. Y. Lee, and Y.-D. Li, “Multiple cracks on the interface between a piezoelectric layer and an orthotropic substrate”, *Acta Mech.* **221** (2011), 297–308.
- [Fil’shtinskii and Fil’shtinskii 1997] L. A. Fil’shtinskii and M. L. Fil’shtinskii, “Anti-plane deformation of a composite piezoceramic space with interphase crack”, *Int. Appl. Mech.* **33** (1997), 655–659.
- [Gao and Wang 2001] C.-F. Gao and M.-Z. Wang, “General treatment of mode III interfacial crack problems in piezoelectric materials”, *Arch. Appl. Mech.* **71** (2001), 296–306.
- [Gao et al. 2001] C.-F. Gao, Y.-T. Zhao, and M.-Z. Wang, “Moving antiplane crack between two dissimilar piezoelectric media”, *Int. J. Solids Struct.* **38** (2001), 9331–9345.
- [Govorukha et al. 2016] V. Govorukha, M. Kamlah, V. Loboda, and Y. Lapusta, “Interface cracks in piezoelectric materials”, *Smart Mater. Struct.* **25** (2016), 023001.
- [Govorukha et al. 2017] V. Govorukha, M. Kamlah, V. Loboda, and Y. Lapusta, *Fracture mechanics of piezoelectric solids with interface cracks*, Lecture Notes in Applied and Computational Mechanics **83**, Springer, Berlin, 2017.
- [Govorukha et al. 2019] V. Govorukha, A. Sheveleva, and M. Kamlah, “A crack along a part of an interface electrode in a piezoelectric bimaterial under anti-plane mechanical and in-plane electric loadings”, *Acta Mech.* **230** (2019), 1999–2012.
- [Häusler et al. 2004] C. Häusler, C.-F. Gao, and H. Balke, “Collinear and periodic electrode-ceramic interfacial cracks in piezoelectric bimaterials”, *J. Appl. Mech. (ASME)* **71** (2004), 486–492.
- [Hou and Mei 1998] M. Hou and F. Mei, “Problems of antiplane strain of electrically permeable cracks between bonded dissimilar piezoelectric materials”, *Chin. Sci. Bull.* **43** (1998), 341–345.
- [Kwon and Lee 2000] J. H. Kwon and K. Y. Lee, “Interface crack between piezoelectric and elastic strips”, *Arch. Appl. Mech.* **70** (2000), 707–714.
- [Kwon and Lee 2001] J. H. Kwon and K. Y. Lee, “Crack problem at interface of piezoelectric strip bonded to elastic layer under anti-plane shear”, *KSME International Journal* **15** (2001), 61–65.
- [Lapusta et al. 2017] Y. Lapusta, O. Onopriienko, and V. Loboda, “An interface crack with partially electrically conductive crack faces under antiplane mechanical and in-plane electric loadings”, *Mech. Res. Commun.* **81** (2017), 38–43.
- [Li and Tang 2003a] X.-F. Li and G. J. Tang, “Antiplane interface crack between two bonded dissimilar piezoelectric layers”, *Eur. J. Mech. A Solids* **22** (2003a), 231–242.
- [Li and Tang 2003b] X.-F. Li and G. J. Tang, “Electroelastic analysis of an interface anti-plane shear crack in a layered piezoelectric plate”, *Int. J. Eng. Sci.* **41** (2003b), 1405–1422.
- [Loboda et al. 2014] V. Loboda, A. Sheveleva, and Y. Lapusta, “An electrically conducting interface crack with a contact zone in a piezoelectric bimaterial”, *Int. J. Solids Struct.* **51** (2014), 63–73.
- [Muskhelishvili 1953] N. I. Muskhelishvili, *Singular integral equations*, Noordhoff Publishers, Groningen, 1953.
- [Nakhmein and Nuller 1988] E. L. Nakhmein and B. M. Nuller, “The pressure of a system of stamps on an elastic half-plane under general conditions of contact adhesion and slip”, *J. Appl. Math. Mech.* **52** (1988), 223–230.
- [Narita and Shindo 1998] F. Narita and Y. Shindo, “Layered piezoelectric medium with interface crack under anti-plane shear”, *Theor. Appl. Fract. Mech.* **30** (1998), 119–126.
- [Narita and Shindo 1999] F. Narita and Y. Shindo, “The interface crack problem for bonded piezoelectric and orthotropic layers under antiplane shear loading”, *Int. J. Fract.* **98** (1999), 87–102.
- [Nourazar and Ayatollahi 2016] M. Nourazar and M. Ayatollahi, “Multiple moving interfacial cracks between two dissimilar piezoelectric layers under electromechanical loading”, *Smart Mater. Struct.* **25** (2016), art. id. 075011.
- [Onopriienko et al. 2019] O. Onopriienko, V. Loboda, A. Sheveleva, and Y. Lapusta, “Bond zone model for a conductive crack at the interface of piezoelectric materials under anti-plane mechanical and in-plane electric loadings”, *Z. Angew. Math. Mech.* **99** (2019), art. id. 201800230.
- [Pak 1992] Y. E. Pak, “Linear electro-elastic fracture mechanics of piezoelectric materials”, *Int. J. Fract.* **54** (1992), 79–100.
- [Park and Sun 1995] S. B. Park and C. T. Sun, “Fracture criteria for piezoelectric ceramics”, *J. Am. Ceram. Soc.* **78** (1995), 1475–1480.
- [Parton and Kudryavtsev 1988] V. Z. Parton and B. A. Kudryavtsev, *Electromagnetoelasticity*, Gordon and Breach Science Publishers, New York, 1988.

- [Ru 2000] C. Ru, “Electrode-ceramic interfacial cracks in piezoelectric multilayer materials”, *J. Appl. Mech. (ASME)* **67** (2000), 255–261.
- [Soh et al. 2000] A. K. Soh, D.-N. Fang, and K. L. Lee, “Analysis of a bi-piezoelectric ceramic layer with an interfacial crack subjected to anti-plane shear and in-plane electric loading”, *Eur. J. Mech. A Solids* **19** (2000), 961–977.
- [Wang 2015] Y.-Z. Wang, “Influences of the remanent polarization and Maxwell stress in surrounding medium on a moving anti-plane crack between two dissimilar piezoelectric solids”, *Theor. Appl. Fract. Mech.* **80** (2015), 253–258.
- [Wang and Sun 2004] B. L. Wang and Y. G. Sun, “Out-of-plane interface cracks in dissimilar piezoelectric materials”, *Arch. Appl. Mech.* **74** (2004), 2–15.
- [Wang and Zhong 2002] X. Wang and Z. Zhong, “A conducting arc crack between a circular piezoelectric inclusion and an unbounded matrix”, *Int. J. Solids Struct.* **39** (2002), 5895–5911.
- [Wang et al. 2003] X. Wang, Z. Zhong, and F. L. Wu, “A moving conducting crack at the interface of two dissimilar piezoelectric materials”, *Int. J. Solids Struct.* **40** (2003), 2381–2399.

VOLODYMYR GOVORUKHA: govorukhavb@yahoo.com

Department of Higher Mathematics and Physics, Dnipro State Agrarian and Economic University, Dnipro, Ukraine

MARC KAMLAH: marc.kamlah@kit.edu

Institute for Applied Materials, Karlsruhe Institute of Technology, Eggenstein-Leopoldshafen, Germany

SHUO ZHAO: xjchina@126.com

School of Mechanical Engineering, Hebei University of Science and Technology, Shijiazhuang, China